Received Date : 27-Apr-2016
Revised Date : 15-Jul-2016
Accepted Date : 11-Aug-2016
Article type : Original Article

Lesion volume predicts prostate cancer risk and aggressiveness: validation of its value alone and matched with PIRADS score.

Article category: Urological Oncology

Eugenio Martorana [a], Giacomo Maria Pirola [a], Michele Scialpi [b], Salvatore Micali [a], Andrea Iseppi [a], Luca Reggiani Bonetti [c], Shaniko Kaleci [d], Pietro Torricelli [e], Giampaolo Bianchi [a]

[a] Urology Department, University of Modena & Reggio Emilia, Modena, Italy.

[b] Department of Surgical and Biomedical Sciences, Division of Radiology 2, Perugia University, S. Maria della Misericordia Hospital, S. Andrea delle Fratte, Perugia, Italy.

[c] Department of Diagnostic Medicine and Public Health, University of Modena and Reggio Emilia - Section of Pathology, Modena, Italy.

[d] Medical Statistic department, University of Modena & Reggio Emilia, Modena, Italy,

[e] Department of Diagnostic Imaging, University of Modena & Reggio Emilia, Modena, Italy

Keywords: PIRADS v2 score, Lesion Volume, Prostate Cancer Detection, Clinical Significant Prostate Cancer, Tumour aggressiveness.

Corresponding author:

Eugenio Martorana, M.D.

Policlinico di Modena, Dept. of Urology,

Via del Pozzo, 71 Modena, 41124, Italy.

Tel. +39 0594223889; Fax +39 059 4222078

E-Mail: *eugeniomartorana@libero.it*

ABSTRACT

Objective: To demonstrate the association between MRI estimated lesion volume (LV), PCa detection and tumour clinical significance evaluating this variable alone and matched with PI-RADSv2 score.

Patients and methods: We retrospectively analysed 157 consecutive patients, with at least one prior negative systematic prostatic biopsy, who underwent transperineal MRI/US fusion targeted biopsy (Tp MRI/US FTB) between January 2014 and February 2016 using Biopsee® system. Suspicious lesions (SL) were bordered using a "region of interest" and the system calculated prostate volume and LV. Patients were divided in groups considering LV (< 0.5 ml, 0.5 - 1 ml, > 1 ml) and PI-RADS score (1-5). We considered as clinically significant PCa (sPCa) all cancers with GS $\geq$ 3 + 4 as suggested by PI-RADS v2. A direct comparison between MRI estimated LV (MRI LV) and histological tumour volume (HTV) was done in 23 patients who underwent radical prostatectomy during the study period. Differences between MRI LV and HTV were assessed using the paired sample t test. MRI LV volume and HTV concordance was verified using a Bland-Altman plot. Chi-square test, logistic and ordinal regression model were used to evaluate difference in frequencies. The selected level of statistical significance was $\leq$ 0.05.

Results: The LV and PI-RADS score were associated both with PCa detection ($p < 0.00001$ and $p= 0.00012$) and with sPCa detection ($p< 0.00001$ and $p= 0.00808$). When the two variables were matched, LV increased the risk within each PI-RADS group. PCa detection became 1.4 times higher

for LV 0.5 - 1 ml and 1.8 times higher for LV > 1 ml; sPCa detection increased 2.6 times for LV 0.5 - 1 ml and 4 times for LV > 1ml. There was positive correlation between MRI LV and HTV (r = 0,9876, p < 0.001). Finally, Bland-Altman analysis showed that MRI LV was underestimated by 4.2% compared to HTV. Study limitations are its monocentric and retrospective design and the limited casistic.

Conclusions: This study demonstrates that PIRADS score and the LV, independently and matched, are associated with PCa detection and with tumour clinical significance.

INTRODUCTION

Currently, multiparametric Magnetic Resonance Imaging (mpMRI) represents the most sensitive imaging modality for Prostate Cancer (PCa) detection [1-3], capable of giving a precise localization of suspected areas within the prostate and guiding clinical decision making for suspected PCa [4].

The European Society of Urogenital Radiology drafted guidelines, including a scoring system, to characterize prostate mpMRI suspected lesions known as PI-RADS™, recently updated to PI-RADS™ v2, to help clinicians in the interpretation and reporting of these findings [5,6].

Literature seems to validate this scoring system, with the advantage of increasing the detection of aggressive tumours (Gleason Score ≥ 7) and to reduce the detection of indolent prostate cancers (iPCa) (GS ≤ 6 and volume < 0.5 ml) compared with random ultrasound-guided (US) biopsies [7].

PI-RADS™ v2 first introduced the value of tumour major diameter compared to the first version. Based on this parameter, a lesion with a given score 4 is upgraded to the higher one when its diameter is more than 15 mm [8]. However, PCa is a solid tumour and has a defined three dimensional shape, so its characteristics are better represented by a volume than a scanned surface.

There is a lack of studies evaluating the role of mpMRI pre-bioptic lesion volume (LV) and its relation to cancer diagnosis and its characteristics.

The aim of this work is to demonstrate the association between suspicious lesion (SL) volume, PCa detection and tumour clinical significance by evaluating this variable alone and matched with PI-RADS™ v2 score.

PATIENTS AND METHODS

Between January 2014 and February 2016, using prostatic mpMRI, we retrospectively evaluated, in the Urology Department of University of Modena and Reggio Emilia (Italy), a cohort of patients with persistent high clinical suspicious for PCa (i.e. persistent elevation of PSA value, suspected DRE, previous diagnosis of ASAP or multifocal HGPIN, combination thereof).

All patients had undergone at least one previous prostate mapping. Specifically, 87 patients (55.4%) had undergone 1 previous prostate mapping; 41 patients (26,1%) had undergone 2 previous prostatic mappings and 29 patients (18.5%) had undergone 3 previous prostate mappings. According with the diagnosis at the previous prostatic mapping: 34 patients (21.7%) had diagnosis of ASAP; 51 patients (32.5%) had diagnosis of HGPIN and 72 patients (45.8%) had diagnosis of BPH/inflammation.

In the study were included 157 patients in which at least one SL or index lesion was detected. These patients were enrolled for transperineal US/MRI fusion targeted biopsy (Tp US/MRI FTB) using BiopSee® system (Tema Sinergie, Germany) [9]. All detected SLs were classified according to the PI-RADSv2 score.

We performed the Tp US/MRI FTB to all patients with at least one SL with PIRADS score ≥2. All patients with only SL PIRADS score 2 were warned of their low risk for cancer diagnosis but they agreed to undertake the procedure. Patients with lesions PIRADS score of 1 were enrolled only if at least one coexistent lesion with PIRADS score ≥ 2 was detected.

Median age was 65.02 (range 47-79 ± 6.8 DS) years, median PSA value was 10.7 ng/ml (range 1.0-75.0 ± 11.29 DS) and median prostate volume was 70.4 ml (range 21-196 ml ± 33.73 DS). Written informed consent was obtained from all participants and a waiver of informed consent was issued to

each patient. An anonymous excel file was created giving a progressive number to each patient.

To standardize the reporting of our data we followed the main statements of the START guidelines [10]. The Table 1 (START Table) summarizes the patients' characteristics and a detailed study flowchart is reported in figure 1.

According with PIRADSv2 criteria [6], outcome measures were reported as follows: a) any PCa, to evaluate the relationship between PIRADS score, LV and PCa detection rate; b) sPCa (GS $\geq 3 + 4$, or pathologically determined tumour volume > 0.5 cc, or pathologically determined extra-prostatic extension) to evaluate the relationship between PIRADS score, LV and sPCa detection.

After PCa diagnosis, data regarding final pathological specimens of patients who underwent RALP during the study period were collected. HTV and MRI LV were compared to verify a correlation between the two measurements.

Finally, early complications as acute urinary retention and perineal hematoma were recorded before the hospital discharge. Moreover, all patients were investigated 20 days after biopsy to collect procedure related late complications (i.e. fever, haematuria, acute urinary retention, perineal hematoma, haemospermia).

Prostatic mpMRI parameters

All mpMRI in this study were performed using a 1.5 Tesla Achieva (Philips Healthcare, Best, The Netherlands) by endorectal (Endorectal MRI-probe, Medrad Performance for Life eCoil) and superficial SENSE cardiac phased-array coil with five channels (Cardiac Synergy Coil, Philiphs Medical Systems, US).

The protocol for prostate MRI included: axial T1-weighted fast spin-echo (FSE) imaging axial, sagittal and coronal T2-weighted FSE imaging, axial DWI (b values of b 0, 350, 700, 1000 s/ mm2) with ADC maps reconstructions, and axial T1-weighted fat-suppression dynamic contrast-enhanced MR imaging (DCE-MRI). T2WI slice thickness and acquisition resolution were 3 mm and 0.5 x 0.5 mm respectively. DCE temporal resolution was 15 sec for 3 minutes (six phases) without breath-

olding, following intravenous single dose injection of 0.2 ml/kg at 2.5 ml/s of gadopentetate dimeglumine (Magnevist; Bayer Schering Pharma AG, Germany). Only a qualitative analysis for DWI and DCE-MRI was carried out.

Two radiologists with 4 years of experience in the field of prostate MRI (P.T. & M.S.), have consensually evaluated mpMRI examinations, searching for the presence of any suspicious area. The index lesion was defined as the largest suspect lesion on axial T2WI and/or DWI/ADC. The axial scan of the DWI/ADC slice containing the greatest suspect area of the index lesion was considered for location matching analysis, and denoted as the apex, middle, or base of the prostate for analyses of three equal trisections of the prostate. Specifically, the centre of the index lesion was defined as the point of intersection of the higher lesion height and width using the lowest ADC value. Finally, the location of the index tumour was recorded according to the 39 PIRADS sectors.

Lesion volume calculation

A preliminary study on T2W MRI images on which are traced the boundaries of the prostate and SL was done in all patients using BiopSee® system.

Considering that the dominant sequence for suspicious lesion in the peripheral zone is the DWI/ADC, the peripheral suspicious lesion is firstly detect on axial DWI/ADC sequence end after on the corresponding axial T2WI. Secondly, axial DWI/ADC and T2WI sequences are imported on BiopSee® system. Then, the axial DWI/ADC sequences are overlapped on the corresponding T2WI one to detect the suspicious lesion on the BiopSee® system. Finally, the radiologist manually traces the suspicious lesion contours only on axial T2W sequences before the MRI/US fusion is done.

Specifically, the boundaries of the SLs are rigorously delimited on the axial plane, using a Region of Interest (ROI) one scan after the other until the entire SL is marked. Each border is automatically and real-time reproduced also on the sagittal and coronal planes by the system obtaining a Volume of Interests (VOI). The volumes of all contoured VOI are automatically calculated. The calculation uses a 3D derivation of Gauss's Theorem algorithm and gives the exact result of the volume

enclosed by the triangulated surface of a VOI. The use of the Gauss's Theorem algorithm implies that the intersecting parts are counted for each involved VOI [11-13]. The calculated volumes, expressed in ml, are displayed in the text field in the upper left corner of the 3D model view. Finally, a graphic three-dimensional representation of the SL within the prostate is done (figure 2)

Pathological analyses of RALP specimens and HTV measurement

After radical prostatectomy, the surgical specimens were fixed in 10% buffered neutral formalin. The prostate surface was inked before the dissection. The prostate was sectioned in three equal trisections named apex, middle and base. Then, routine hematoxylin and eosin stained serial 3 µm thickened slides were obtained from each trisection.

Index tumour was defined as the largest tumour focus taking into account Gleason score.

The HTV measurement was obtained for the index tumour as follow. The tumour length maximum diameter was defined as the largest tumour dimension on any cross-section. Tumour width was considered as the maximal width perpendicular to the tumour length maximum diameter. The tumour thickness was calculated as the number of slices containing index tumour multiplied by the average slice thickness of the respective specimen. All measures were performed without a correction factor as described by Baco et al. [14]. According with Perera et al the HTV was calculated via an ellipsoid volume formula using the longest perpendicular diameters: depth x width x length x 0.523 [15].

Figure 3 shows the comparison between radiological SL in axial plane and the appearance of the corresponding pathological confirmed tumour (figure 3).

The pathology slide with the greatest cross-section of the index tumour was used for location matching analysis. The centre of the index tumour was defined as the point of intersection of the lesion height and width dimensions and the location of the index tumour was recorded according to the 39 PIRADS sectors.

Bioptic Technique

BiopSee® is a system designed to perform Tp US/MRI FTB. All Tp US/MRI FTB were performed by a single experienced urologist (E.M.) under general anaesthesia to ensure the patient's immobility. Even if anaesthesia is not the standard practice for this procedure type, Tp US/MRI FTB is a highly accurate procedure. Thus, all small patient movements (i.e. voluntary movements of the chest, cough, sneezing, speech, etc) are inevitably reflected on the pelvis and could jeopardize the goodness of fusion, once it has been done, affecting the benefits of the procedure.

An US scan of the prostate was performed in cranio-caudal direction in order to acquire the entire axial 2D prostate volume. Biopsee® then reworked these sequences to provide a 3D US reconstruction of the gland on which perform US/MRI images fusion with T2W sequences previously imported and bordered (figure 4). Tp US/MRI FTB was done on any SL followed by a further 24 random samples using the Ginsburg Study Group scheme [16]. The needle, inserted through the transperineal template, passes through the prostate along a longitudinal trajectory until the target area was reached. Samples were obtained with a 18G × 16 cm disposable needle biopsy, mounted on a reusable biopsy gun (Pro-Mag Ultra®, Angiotech, Denmark) (Figure 5). All samples were collected in blocks named according to the sampling area and sent separately for histopathological examination. Following each biopsy, the exact 3D pickup location was recorded and stored by the software.

Statistical Analysis

Data were analysed by statistical package STATA13 (StataCorp. 2011. Stata: Release 12 Statistical Software. College Station, TX: StataCorp LP). Differences between MRI LV volume and HTV were assessed using the paired sample t test. MRI LV and HTV concordance was verified using a Bland-Altman plot. Chi-square test, logistic and ordinal regression model were used to evaluate difference in frequencies. Continuous variables were expressed as mean ± standard deviation and range. The selected level of statistical significance is equal to 0.05.

RESULTS

Overall detection rate was 50.32% (79/157 patients): 52 patients (65.83%) had PCa detected on targeted biopsy only, 18 (22.78%) on systematic biopsy only (total number of positive random core in these patients was 38), and 9 (11.39%) on both targeted and systematic biopsy ($p< 0.00001$). All the sPCa were detected by Tp US/MRI FTB. Table 2 show the GS distribution considering both targeted and random biopsies.

Detected SL were 283 (range 1-4, median 1.83). LV ranged from 0.02 to 12 ml (median 0.67 ± 1.18 DS). According to LV, the SLs were divided in three groups: 168 with LV < 0.5 ml, 71 between 0.5 and 1 ml and 44 > 1 ml. Moreover, 6 SLs were classified as PIRADS 1, 108 as PIRADS 2, 75 as PIRADS 3, 66 as PIRADS 4 and 28 as PIRADS 5.

Histologically, PCa confirmed SLs were 74/283 (26.15%). Table 3 summarizes the SL characteristics matching their PIRADS score and LV and crosses them considering the histological result as positive or negative. Figure 6 shows the LV distribution according to their histological results.

PCa detection rate increased with the PIRADS score rising from 0% to 2.8% (3/108) to 12% (9/75), to 57.6% (38/66) and to 85.7% (24/28) for PIRADS score 1, 2, 3, 4 and 5 respectively ($p < 0.00001$). Using a univariate logistic regression model and considering PIRADS 1 plus PIRADS 2 as comparison group we found that PCa was 5 times higher for PIRADS 3, becomes 50 times higher for PIRADS 4 and 222 times higher for PIRADS score 5 lesions.

PCa diagnosis also increased with the increase of LV from 17.3% (29/168) to 35.2% (25/71) to 45.5% (20/44) when LV was ≤ 0.5 ml, between 0.5 and 1 ml and ≥ than 1 ml respectively ($p=0.00012$). Using a univariate logistic regression model and considering 0.5 ml LV as a comparison group, we found that PCa risk was 2.6 times higher for LV between 0.5 and 1 ml and 4 times higher for LV > 1ml. Finally, using an ordinal logistic regression model and considering

lesions < 0.5 ml as comparison group, we found that, within each PIRADS lesions group, the probability of finding a PCa is 1.4 times higher when LV is between 0.5 and 1 ml and becomes 1.8 times higher when LV is more than 1 ml.

Table 4 shows PCa confirmed lesions and reports the relationship between their volume and the bioptic GS. The sPCa were 25/74 (33.8%) compared to 49/74 (66.2%) in which GS was ≤ 6 (p= 0.022). Considering LV, the sPCa detection rate was as follows (Table 4): 4/29 tumours (13.8%) with volume < 0.5 ml, 10/25 tumours (40%) with volume between 0.5 and 1 ml and 11/20 tumours (55%) with a volume > 1 ml (p= 0.00808). Figure 7 shows the LV distribution according with their GS.

Considering the PIRADS score, the sPCa detection rate was as follows (Table 5): (0%) PIRADS score 1, 0/6 (0%) PIRADS score 2, 1/9 (1.1%) PIRADS score 3, 11/38 (28.9%) PIRADS score 4, 13/24 (54.2%) PIRADS score 5 (p= 0.03). Moreover, Table 6 shows the association between sPCa diagnosis and the two variables (i.e. PIRADS score and LV) when matched. Using an ordinal logistic regression model and considering lesions < 0.5 ml as a comparison group, we found that, within each PIRADS lesions group, the probability of detecting a higher GS (≥7) is 3.5 times higher when LV is between 0.5 and 1 ml and becomes 4.3 times higher when LV is more than 1 ml. Moreover, Table 6 allows to identify the sPCa detection rate based on each PIRADS and LV groups. In fact, considering the SL group with the LV ≤ 0.5 ml, sPCa detection was 0% for SLs with PIRADS 1,2 and 3; it increased to 3/32 (9.4%) for SLs PIRADS 4 and becomes 1/5 (20%) for SLs PIRADS 5 (p=0.002). Considering the SL group with LV between 0.5 and 1 ml, sPCa detection was 0% for SLs with PIRADS 1,2 and 3; increased to 5/26 (19.2%) for SLs PIRADS 4 and becomes 5/10 (50%) for SLs PIRADS 5 (p= 0.0007). Finally, considering SL group with LV ≥ 1ml, sPCa detection was 0% for SLs with PIRADS score 1 and 2, 1/14 (7.1%) for SLs PIRADS 3, increases to 3/8 (37.5%) for PIRADS 4 lesions and reaches 7/13 (53.8%) for SLs PIRADS 5 (p=0.008).

Similarly to what reported for PIRADS score, the sPCa detection rate proportionally increased with the increase of LV considering the same PIRADS score, even if statistical significance was not

achieved with our data. For example, considering PIRADS 4 lesions group, sPCa detection was 3/32 (9.4%) for lesions ≤0.5 ml, increased to 5/26 (19.2%) for lesion between 0.5 and 1 ml and becomes 3/8 (37.5%) for lesions > 1ml (p= 0.1).

No severe post-operative complications were collected: 3.2% of patients reported moderate haematuria, 5.7 % had an acute urinary retention, 11.46 % reported perineal hematoma and 86% referred haemospermia. Neither fever nor urinary sepsis were reported (0%).

Twenty-three/61 patients (37.7%) underwent robot-assisted laparoscopic radical prostatectomy (RALP). The risk to have a locally extended (pT2c) or advanced (≥ pT3a) PCa became statistically significant for radiologic LV > 0.5 ml (p= 0.025 and p=0.045 respectively) (Table 7).

Finally, the direct comparison between pathological and radiological findings was done. The mean index MRI LV was 0.94 ml (range 0.12–3.8 ml) and the mean index HTV was 1.13 ml (range 0.12–4.4 ml). Three index tumours (13%), incidentally detected by systematic biopsy, were invisible on MRI. The mean volume for these tumours was < 0.3 ml. The remaining 20 index tumours (87%) were visible on MRI. A correspondence of 100% between mpMRI findings and pathological locations of the tumour was observed. There was positive correlation between MRI LV and HTV (r = 0,9876, p < 0.001). Bland-Altman analysis reveals clinically significant bias in the agreement between MRI LV and HTV. MRI LV was underestimated by 4.2% [95% CI (2% - 8.2%)] compered to HTV (figure 8).

DISCUSSION

Multiparametric MRI (mpMRI) is an evolution of standard MRI and it is demonstrated that its clinical application helps to manage suspected and proved prostate cancer [17].

MpMRI increases the clinic diagnostic yield of prostate cancer compared to US, with a proved correlation between PIRADS score and tumour detection, while correlation between PIRADS score and tumour aggressiveness is still debatable [18,19].

When used to perform Fusion Targeted Biopsy (FTB), mpMRI is demonstrated to increase diagnostic yield for sPCa compared to simple transrectal US guided biopsy [20-22].

As the volume of a cancerous lesion is increasingly incorporated into sPCa definitions, a crucial issue is the correct estimation of TV by mpMRI [23]. In fact, the valuation of LV before biopsy should add important informations to understand the risk of lesion itself, to identify the patients in which FTB is required and to make the correct decision once the bioptic PCa diagnosis is done.

A number of studies has evaluated the correspondence between mpMRI LV and HTV on a radical prostatectomy specimen [14, 24] finding a positive correlation with an underestimation of mpMRI LV ranged from 5.9% (without shrinkage factor) to 20% (using a shrinkage factor of 1.15). In our study we compared MRI LV and HTV measurement without considering a correction factor and the results were stackable with those obtained by Baco et al [14].

As proved by many authors [18-20] our study confirm that cancer detection rate increased with increase of PIRADS score being statistically significant higher for ≥ PIRADS 4 lesions. We found that probability to diagnose a PCa increase from 5 to 50 times switching from PIRADS 3 to 4 and became 222 times higher for PIRADS 5 lesions. Similarly to PIRADS score, cancer detection rate independently increased with increase of LV being statistically significant higher for SL > 1 ml. We found that the probability to diagnose a PCa is 2.6 times higher for LV between 0.5 and 1 ml and became to 4 times higher for LV > 1 ml. Moreover, matching PIRADS score and LV we found that, within each PIRADS lesions group, the probability to diagnose PCa increased proportionally with LV increase.

Another concept is the sPCa detection predictability of mpMRI, still debatable by many authors [18, 26, 27]. Our study shows that sPCa diagnosis significantly increase both with PIRADS score increase (see Table 5), and with LV rise (see Table 4). This evidence should be related to the aggressive tumour biology with a quickly grow and so a high probability to find a large LV at mpMRI.

Table 6, that we define PiVoGle table, matches PIRADS score, LV and GS and allow to define the correlation between sPCa detection and the two variables when matched. We found that, at PIRADS score increase, the probability to detect a higher GS (≥7) proportionally increases with LV increase. According with Table 6 data, we can state that lesions with PIRADS score ≤ 2 should not be sampled (PCa detection rate= 2.8% with a iPCa diagnosis in all cases) and that patients with lesion PIRADS score 3 and MRI LV < 0.5 ml should be informed of low PCa risk (PCa detection = 10.42 % with a iPCa diagnosis in all cases). Liddell H et al [19] based on Epstein criteria concluded that PIRADS 3 lesions should not be sampled but surveilled only because these lesions are associated with a low risk of sPCa. The results of our study, in agreement with those of the Baco et al. [14] showed a positive correlation between MRI LV and HTV confirming that mpMRI not overestimate but rather underestimates the true HTV. Based on these principles we believe that MRI LV can be discriminant for PIRADS score 3 SL group and, including MRI LV as sPCa criteria, we found that 14.8% of PIRADS 3 and > 0.5 ml lesions results in a sPCa. So, in our opinion MRI LV can aid clinicians to understand what SL should undergo FTB.

Finally, Wolters T et al reported a positive relationship between tumour volume > 0.5 ml at radical prostatectomy, PCa staging and Gleason score [27]. Likewise, although our still small RALP series, we found that mpMRI LV has an independent correlation with tumour local extension and a LV > 0.5 ml was significantly associated both with a local extended PCa and with a local advanced PCa.

The limits of this study is its retrospective design. Moreover, data are related to a single centre and to a limited casistic and therefore cannot be considered conclusive. These findings should be applied to a multicentric and larger cohort of patients to be validated or to assess the definitive PCa risk for each lesions group. Finally, no shrinkage factor was applied to normalize the underestimation of mpMRI LV. Nevertheless, clinical application of our tables should help urologists to determinate PCa risk of each patient based on mpMRI SL characteristics.

CONCLUSION

Our experience with Tp US/MRI FTB has demonstrated substantial advantages in terms of overall detection rate and increase of sPCa. This study demonstrates that PIRADS score and LV, independently and matched, are associated with PCa detection and with tumour clinical significance.

ACKNOWLEDGMENTS

We thank Mr Jonathan Brereton Jones from Linguistic centre of the University of Modena and Reggio Emilia for his help in the article English revision.

ABBREVIATION LIST

aPCa: aggressive cancer

DCE: dynamic contrast-enhanced

DWI: diffusion weighted imaging

FSE: fast spin-echo

FTB: fusion targeted biopsy

GS: Gleason score

HTV: histological tumour volume

iPCa: indolent prostate cancers

LV: lesion volume

MRI LV: Magnetic Resonance Imaging estimed lesion volume

mpMRI: multiparametric Magnetic Resonance Imaging

PI-RADS: Prostate Imaging Reporting and Data System

PCa: prostate cancer

PSA: prostatic specific antigen

ROI: region of interest

RALP: robot-assisted laparoscopic radical prostatectomy

sPCa: significant prostate cancer

SL: suspicious lesion

Tp US/MRI FTB: trans-perineal ultrasound/magnetic resonance imaging fusion targeted biopsy

TV: tumour volume

US: ultrasound

VOI: volume of interest

REFERENCES

[1] Fütterer JJ, Briganti A, De Visschere P, et al. Can Clinically Significant Prostate Cancer Be Detected with Multiparametric Magnetic Resonance Imaging? A Systematic Review of the Literature. Eur Urol. 2015 Dec;68(6):1045-53.

[2] Hoeks CM, Barentsz JO, Hambrock T, et al. Prostate cancer: multiparametric MR imaging for detection, localization, and staging. Radiology 2011;261:46–66.

[3] Delongchamps NB, Beuvon F, Eiss D, et al. Multiparametric MRI is helpful to predict tumor focality, stage, and size in patients diagnosed with unilateral low-risk prostate cancer. Prostate Cancer Prostatic Dis 2011;14:232–7.

[4] Delongchamps NB, Rouanne M, Flam T, et al. Multiparametric magnetic resonance imaging for the detection and localization of prostate cancer: combination of T2-weighted, dynamic contrast-enhanced and diffusion-weighted imaging. BJU Int 2011;107: 1411–8.

[5] Hamoen EHJ, De Rooij M, Witjes JA, Barentsz JO, Rovers MM. Use of the Prostate Imaging Reporting and Data System (PI-RADS) for prostate cancer detection with multiparametric magnetic resonance imaging: a diagnostic meta-analysis. Eur Urol 2015;67:1112–21.

[6] Weinreb JC, Barentsz JO, Choyke PL, et al. PI-RADS Prostate Imaging - Reporting and Data System: 2015, Version 2. Eur Urol. 2016 Jan;69(1):16-40.

[7] Schoots IG, Roobol MJ, Nieboer D, Bangma CH, Steyerberg EW, Hunink MG. Magnetic resonance imaging-targeted biopsy may enhance the diagnostic accuracy of significant prostate cancer detection compared to standard transrectal ultrasound-guided biopsy: a systematic review and meta-analysis. Eur Urol. 2015 Sep;68(3):438-50.

[8] Barentsz JO, Weinreb JC, Verma S et al: Synopsis of the PI-RADS v2 Guidelines for Multiparametric Prostate Magnetic Resonance Imaging and Recommendations for Use. Eur Urol 2016; 69: 41-49

[9] Hansen N, Patruno G, Wadhwa K, et al. Magnetic Resonance and Ultrasound Image Fusion Supported Transperineal Prostate Biopsy Using the Ginsburg Protocol: Technique, Learning Points, and Biopsy Results. Eur Urol. 2016 Aug;70(2):332-40. doi: 10.1016/j.eururo.2016.02.064. Epub 2016 Mar 16.

[10] Moore CM, Kasivisvanathan V, Eggener S, et al; START Consortium. Standards of reporting for MRI-targeted biopsy studies (START) of the prostate: recommendations from an International Working Group. Eur Urol. 2013 Oct;64(4):544-52. doi: 10.1016/j.eururo.2013.03.030. Epub 2013 Mar 20.

[11] Matyka M, Ollila MA. Pressure Model for Soft Body Simulation. Proc. of Sigrad, UMEA, Nov 2003.

[12] Ancona MG. Computational Methods for Applied Science and Engineering: An interactive Approach. Rinton Press, 2002.

[13] Matyka M. How To Implement a Pressure Soft Body Model. maq@panoramix.ift.uni.wroc.pl March 30, 2004.

[14] Baco E, Ukimura O, Rud E, et al. Magnetic resonance imaging-transectal ultrasound image-fusion biopsies accurately characterize the index tumor: correlation with step-sectioned radical prostatectomy specimens in 135 patients. Eur Urol. 2015 Apr;67(4):787-94.

[15] Perera M, Lawrentschuk N, Bolton D, Clouston D. Comparison of contemporary methods for estimating prostate tumour volume in pathological specimens. BJU Int. 2014 Mar;113 Suppl 2:29-34. doi: 10.1111/bju.12458.

[16] Kuru TH, Wadhwa K, Chang RT et al. Definitions of terms, processes and a minimum dataset for transperineal prostate biopsies: a standardization approach of the Ginsburg Study Group for Enhanced Prostate Diagnostics. BJU Int 2013; 112: 568-577.

[17] Le JD, Tan N, Shkolyar E, et al. Multifocality and prostate cancer detection by multiparametric magnetic resonance imaging: correlation with whole-mount histopathology. Eur Urol. 2015 Mar;67(3):569-76.

[18] Cash H, Maxeiner A, Stephan C et al: The detection of significant prostate cancer is correlated with the Prostate Imaging Reporting and Data System (PI-RADS) in MRI/transrectal ultrasound fusion biopsy. World J Urol 2016 Apr;34(4):525-32.

[19] Liddell H, Jyoti R, Haxhimolla HZ. mp-MRI Prostate Characterised PIRADS 3 Lesions are Associated with a Low Risk of Clinically Significant Prostate Cancer- A Retrospective Review of 92 Biopsed PIRADS 3 Lesions. Curr Urol 2015; 8: 96-100

[20] Valerio M, Donaldson I, Emberton M et al. Detection of Clinically Significant Prostate Cancer Using Magnetic Resonance Imaging-Ultrasound Fusion Targeted Biopsy: A Systematic Review. Eur Urol 2015; 68: 8-19

[21] Siddiqui MM, Rais-Bahrami S, Truong H, et al. Magnetic resonance imaging/ultrasound-fusion biopsy significantly upgrades prostate cancer versus systematic 12-core transrectal ultrasound biopsy. Eur Urol. 2013 Nov;64(5):713-9.

[22] Martorana E, Micali S, Ghaith A, et al. Advantages of single-puncture transperineal saturation biopsy of prostate: analysis of outcomes in 125 patients using our scheme. Int Urol Nephrol. 2015 May;47(5):735-41.

[23] Wolters T, Roobol MJ, van Leeuwen PJ, et al. A critical analysis of the tumor volume threshold for clinically insignificant prostate cancer using a data set of a randomized screening trial. J Urol 2011; 185:121–5

[24] Radtke JP, Schwab C, Wolf MB, et al. Multiparametric Magnetic Resonance Imaging (MRI) and MRI-Transrectal Ultrasound Fusion Biopsy for Index Tumor Detection: Correlation with Radical Prostatectomy Specimen. Eur Urol. 2016 Jan 19.

[25] Litjens GJ, Barentsz JO, Karssemeijer N, Huisman HJ. Clinical evaluation of a computer-aided diagnosis system for determining cancer aggressiveness in prostate MRI. Eur Radiol. 2015 Nov;25(11):3187-99.

[26] Dwivedi DK, Kumar R, Bora GS, et al. Stratification of the aggressiveness of prostate cancer using pre-biopsy multiparametric MRI (mpMRI). NMR Biomed. 2016 Mar;29(3):232-8.

[27] Wolters T, Roobol MJ, van Leeuwen PJ, et al. Should Pathologists Routinely Report Prostate tumour volume? The prognostic value of tumour volume inprostate cancer. Eur Urol. 2010 May;57(5):821-9.

LEGENDS TO ILLUSTARTIONS

Figure 1. Study flowchart

Figure 2. Suspicious lesion affecting the left peripheral zone of the prostate. Boundaries of the SL are rigorously delimited in axial plane(C), using a Region of Interest (ROI) one scan after the other until the entire SL is marked. Each border is automatically and real-time reproduced also on the sagittal (B) and coronal (A)planes by the system obtaining a Volume of Interests (VOI).The system automatically calculates both the prostate and suspicious lesion volumes giving a value in ml (D).

Figure 3. Comparison between MRI SL and pathological confirmed tumor. A) Contouring of the MRI SL in axial plane by BiopSee Sistem ®. B) Contouring of the pathological confirmed tumor in the corresponding slide (slices were stained with haematoxylin-eosin after being embedded in paraffin).

Figure 4. Suspicious lesion affecting the anterior zone of the prostate. In this figure, US/MRI fusion was performed and the obtained MRI VOI was overlapped to the equivalent US scan. Histopathological examination revealed a GS 7 (3+4) prostate cancer in all targeted cores.

Figure 5. PRO-MAG ultra ®. It is an automatic and reusable biopsy gun for histological core biopsies: A) Needle allocation system; B) Biopsy gun ready for use; C) The needle has an echogenic tip for accurate placement under ultrasound guidance; D) Biopsy core.

Figure 6. Boxplot representation of LV distribution according with their positive or negative histological results. For negative SL volume median value was 0.37, for positive SL volume median value was 0.59.

Figure 7. Boxplot representation of LV distribution according with their Gleason Score.

A. LV distribution considering non-aggressive (GS≤6) and aggressive (GS≥7) tumors
B. LV distribution inside each GS groups

Figure 8. (A) Scatter plot showing correlation between MRI estimated tumor volume (mpMRI LV) and histological tumor volume (HTV) in 23 patients. The red line indicates the regression line.
(B) Bland-Altman plot showing the limitation of agreement between mpMRI LV and HTV. The orange line represents the linear regression line. The percentage difference between mpMRI LV and HTV is plotted against the average tumor volume (calculated from both mpMRI LV and HTV). All values above the zero line represent overestimation of mpMRI LV, and all values below the zero line represent underestimation of mpMRI LV. The average underestimation of HTV by MRI is 4.2% (95%CI [2% - 8.2%]), and is constant throughout the measurement range. The limit of agreement ranges from -0.54 to +0.15, which indicates clinically significant inaccuracy for mpMRI LV. The median (range) is 0.72 ml (0.12–3.8 ml) for mpMRI LV and 0.89 ml (0.12–4.4 ml) for HTV. Graphic generated using MedCalc Software bvba Version 16.4.3.

TABLES AND THEIR LEGENDS

Table 1. START table showing pre-biopsy patients characteristics (n=157), mpMRI findings, biopsy cores and RALP outcomes (n= 23)

Men included in analysis, *n*	157
Age, yr, median (IQR)	65 (47 - 79)
Pre-biopsy PSA level, ng/ml, median (IQR)	10,7 (1 - 75,0)
Suspicious DRE findings (≥T2), *n* (%)	12 (8%)
Prostate volume, ml, median (IQR)	70,40 (21,00 - 196,56)
PSA density, median, (IQR)	0,18 (0,04 - 1,32)
Patients with prior prostate biopsy, *n* (%)	157 (100%)
Patients without prior biopsy, *n* (%)	0 (0%)
Patients with 1 prior biopsy	87
Patients with 2 prior biopsy	41
Patients with 3 prior biopsy	29
Number of cores in prior biopsy, median (IQR)	17 (12 - 36)
Patients undergoing active surveillance, *n* (%)	0 (0%)
Days from mpMRI to biopsy, median (IQR)	52 (30-78)
Days from mpMRI to radical prostatectomy, median (IQR)	74 (50 - 90)
Men with PI-RADS ≥2 lesions on mpMRI, *n* (%)	157 (100%)
Number of lesions PI-RADS ≥2	277 (98%)
Patients with one PI-RADS ≥2 lesion	74
Patients with two PI-RADS ≥2 lesions	51
Patients with three or more PI-RADS ≥2 lesions	32
Overall PI-RADS score 2 lesions, *n* (% of PI-RADS ≥2)	108 (39%)
Overall PI-RADS score 3 lesions, *n* (% of PI-RADS ≥2)	75 (27%)
Overall PI-RADS score 4 lesions, *n* (% of PI-RADS ≥2)	66 (24%)
Overall PI-RADS score 5 lesions, *n* (% of PI-RADS ≥2)	28 (10%)
Biopsies per patient, median (IQR)	28 (26 - 34)
Systematic biopsies per patient, median (IQR)	24 (24 - 24)
Targeted biopsies per patient and per lesion, median (IQR)	4 (2 - 10), 2.5 (1-5)
Overall lesions in radical prostatectomy specimen, *n*	32
Index tumour lesions, *n*	23
Additional lesions, *n*	9
Patients with additional lesions, *n* (%)	5 (22%)

Table 2: Gleason Score distribution considering both targeted (horizontally) and random biopsies (vertically).

		Random						***Total***
		Negative	**Gl 6 (3+3)**	**Gl7 (3+4)**	**Gl 7 (4+3)**	**Gl 8 (4+4)**	**Gl 8 (5+3)**	
Targeted	**Negative**	78	18	0	0	0	0	96
	Gl 6 (3+3)	29	9	0	0	0	0	38
	Gl 7 (3+4)	11	0	0	0	0	0	11
	Gl 7 (4+3)	5	0	0	0	0	0	5
	Gl 8 (4+4)	5	0	0	0	0	0	5
	Gl 8 (5+3)	2	0	0	0	0	0	2
Total		130	27	0	0	0	0	157

Table 3: PIVo Table summarizes SL characteristics matching their PIRADS score, LV and histological results (positive or negative). With this table is possible understand the additional value of LV when the two variables are matched. For example, in our study PCa detection rate for SLs group with PIRADS score 3 and volume between 0.5 and 1 ml was 1 (positive lesion)/1 (positive lesion) +12 (negative lesions) = 7.7%). The PCa detection rate was significantly higher for SLs group with the same PIRADS score and LV > 1 (3 (positive lesion) /3 (positive lesion) + 11 (negative lesion) = 21.4%).

VOLUME	**POSITIVE**					**Sub Tot**	**NEGATIVE**					**Sub Tot**	**TOT**	**P**
	PIRADS V2 score						**PIRADS V2 score**							
	1	**2**	**3**	**4**	**5**		**1**	**2**	**3**	**4**	**5**			
≤ 0,5 ml	0	3	5	17	4	***29***	6	74	43	15	1	*139*	***168***	PIRADS score < 0.00001 VOLUME = 0.00012
0,5 < x< 1 ml	0	0	1	15	9	***25***	0	22	12	11	1	*46*	***71***	
≥ 1 ml	0	0	3	6	11	***20***	0	9	11	2	2	*24*	***44***	
TOTAL	***0***	***3***	***9***	***38***	***24***	***74***	***6***	***105***	***66***	***28***	***4***	***209***	***283***	

Table 4: VoGle Table. Positive SL were grouped considering Volume and Gleason Score (GS). Aggressive tumor rate (GS≥7) increased with increase of LV

VOLUME	**POSITIVE**					**TOTAL**	**p**
	GS 6 (3+3)	**GS 7 (3+4)**	**GS 7 (4+3)**	**GS 8 (4+4)**	**GS 8 (5+3)**		
≤ 0,5 ml	25	2	2	0	0	*29*	***0.00808***
0,5 < x< 1 ml	15	6	1	3	0	*25*	
≥ 1 ml	9	3	2	4	2	*20*	
TOTAL	***49***	***11***	***5***	***7***	***2***	***74***	

Table 5: PIGle Table reports the relationship between PIRADS score and bioptic Gleason Score. Tumor aggressiveness increased with the increase of PIRADS score.

PI-RADS$_{V2}$	POSITIVE					TOTAL	p
	GL 6 (3+3)	GL 7 (3+4)	GL 7 (4+3)	GL 8 (4+4)	GL 8 (5+3)		
1	0	0	0	0	0	*0*	***p =0.03***
2	3	0	0	0	0	*3*	
3	8	1	0	0	0	*9*	
4	27	5	2	3	1	*38*	
5	11	5	3	4	1	*24*	
TOTAL	***49***	***11***	***5***	***7***	***2***	***74***	

Table 6: PiVoGle table matches PIRADS score, lesion volume and GS.
This table permits to calculate the PCa and sPCa risk of each lesion considering its PIRADS score and volume. For example the PCa risk of a lesion with PIRADS score 4 and LV between 0.5 ml and 1 ml is 15/26= 57.7% and its sPCa risk is 5/26= 19.2% and so on.

PI-RADS v2	n°	VOL (ml)	POSITIVE					Sub Tot	NEGATIVE	TOT
			GL 6 (3+3)	GL 7 (3+4)	GL 7 (4+3)	GL 8 (4+4)	GL 8 (5+3)			
1	6	**≤ 0.5**	0	0	0	0	0	*0*	6	***6***
		0.5 <x< 1	0	0	0	0	0	*0*	0	***0***
		≥ 1	0	0	0	0	0	*0*	0	***0***
2	108	**≤ 0.5**	3	0	0	0	0	*3*	74	***77***
		0.5 <x< 1	0	0	0	0	0	*0*	22	***22***
		≥ 1	0	0	0	0	0	*0*	9	***9***
3	75	**≤ 0.5**	5	0	0	0	0	*5*	43	***48***
		0.5 <x< 1	1	0	0	0	0	*1*	12	***13***
		≥ 1	2	1	0	0	0	*3*	11	***14***
4	66	**≤ 0.5**	14	1	2	0	0	*17*	15	***32***
		0.5 <x< 1	10	3	0	2	0	*15*	11	***26***
		≥ 1	3	1	0	1	1	*6*	2	***8***
5	28	**≤ 0.5**	3	1	0	0	0	*4*	1	***5***
		0.5 <x< 1	4	3	1	1	0	*9*	1	***10***
		≥ 1	4	1	2	3	1	*11*	2	***13***
TOTAL			***49***	***11***	***5***	***7***	***2***	***74***	***209***	***283***

Table 7: Relationship between lesion volume and final pathological specimen. LV > 0.5 ml is significantly associated both with local extended prostate cancer and with local advanced prostate cancer when compared with final specimens.

Stadiation after RALP	**Bioptic GS**	**Lesion Volume (ml)**	**p**
pT2a GS (3+3)	6 (3+3)	< 0.5	
	6 (3+3)	< 0.5	
	6 (3+3)	< 0.5	
pT2c GS 6 (3+3)	6 (3+3)	0.5 ≤ X ≤ 1	
	6 (3+3)	0.5 ≤ X ≤ 1	
	6 (3+3)	< 0.5	**Extended PCa = 0.025**
	6 (3+3)	0.5 ≤ X ≤ 1	
	6 (3+3)	< 0.5	
	6 (3+3)	< 0.5	
pT2c GS (3+4)	6 (3+3)	0.5 ≤ X ≤ 1	
	7 (3+4)	0.5 ≤ X ≤ 1	
pT2c GS (4+3)	7 (4+3)	>1	
	7 (4+3)	< 0.5	
pT3a GS 6 (3+3)	6 (3+3)	< 0.5	
	6 (3+3)	>1	
	6 (3+3)	>1	**Advanced PCa = 0.045**
pT3a GS7 (3+4)	6 (3+3)	< 0.5	
pT3a GS 7(4+3)	*7 (3+4)*	0.5 ≤ X ≤ 1	
	7(4+3)	>1	
pT3a GS 8 (3+5)	*8 (5+3)*	>1	
pT3b GS 6 (3+3)	*6 (3+3)*	0.5 ≤ X ≤ 1	
pT3b GS 7 (4+3)	8 (4+4)	>1	
pT3b GS9 (4+5), N1	8 (4+4)	>1	

Figure 1. Study flowchart

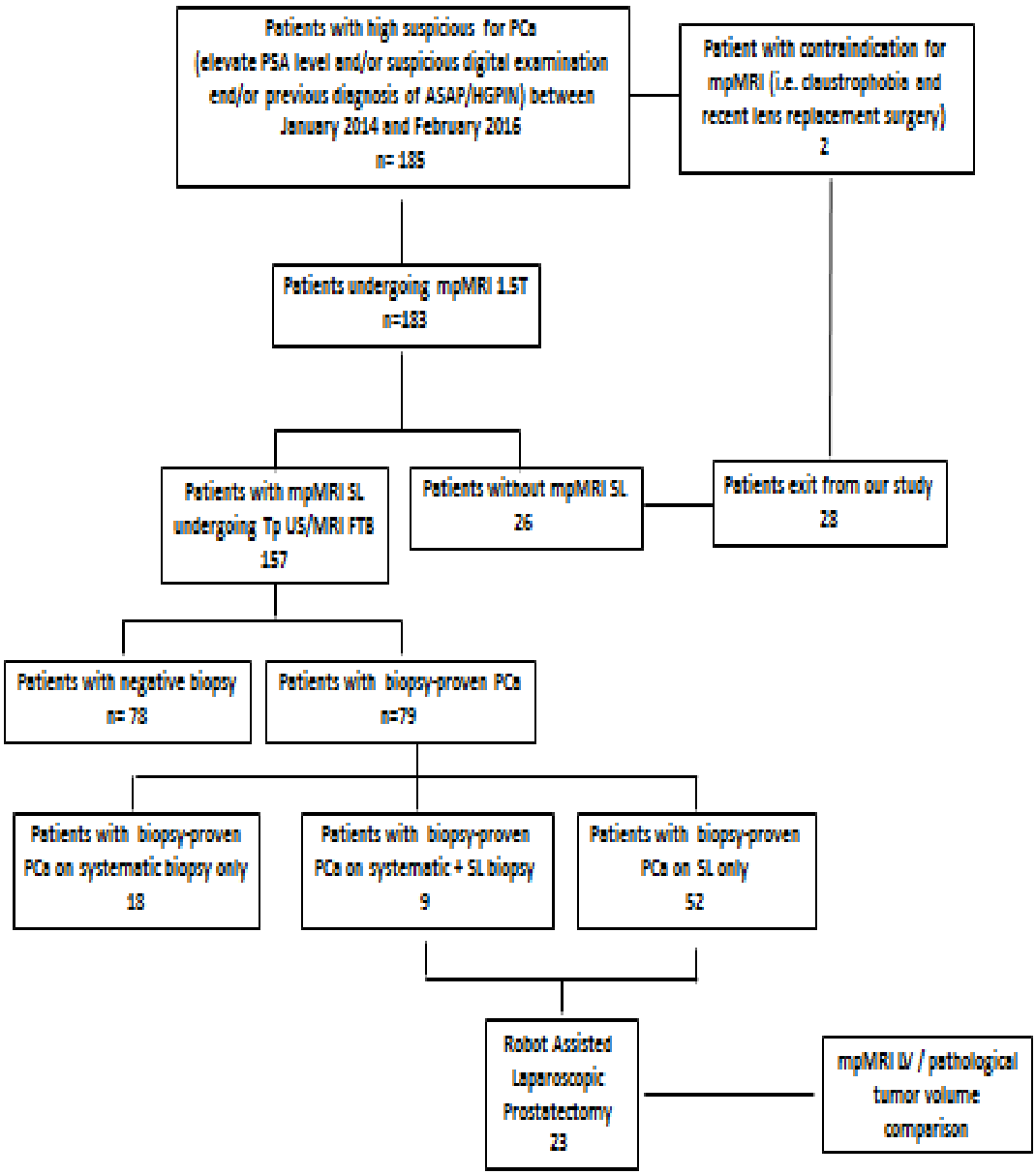

Figure 2. **Suspicious lesion affecting the left peripheral zone of the prostate.** Boundaries of the SL are rigorously delimited in axial plane(C), using a Region of Interest (ROI) one scan after the other until the entire SL is marked. Each border is automatically and real-time reproduced also on the sagittal (B) and coronal (A) planes by the system obtaining a Volume of Interests (VOI). The system automatically calculates both the prostate and suspicious lesion volumes giving a value in ml (D).

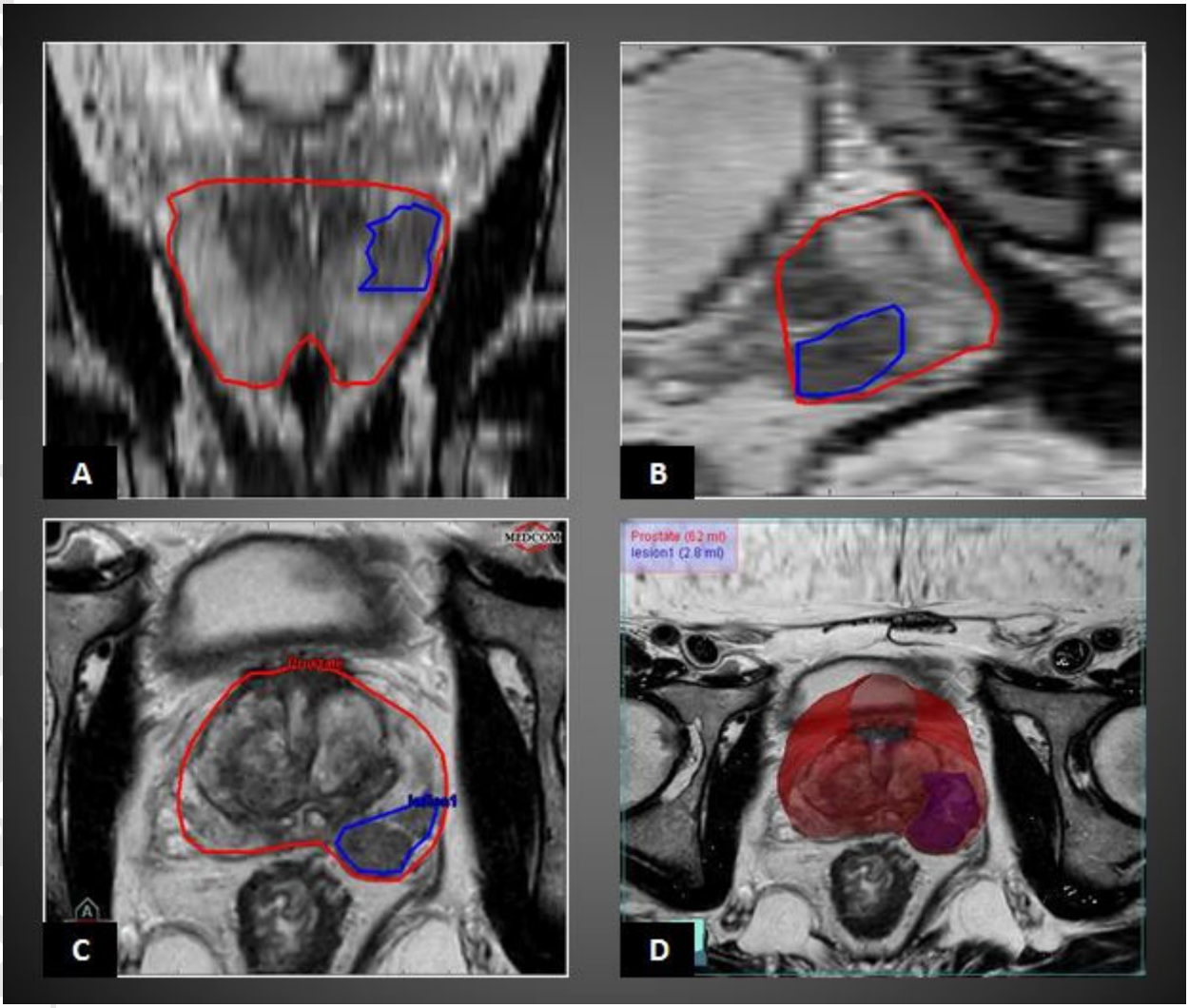

Figure 3: Comparison between MRI SL and pathological confirmed tumor. A) Contouring of the MRI SL in axial plane by BiopSee Sistem ®. B) Contouring of the confirmed tumour in the pathological corresponding slide (slices were stained with haematoxylin-eosin after being embedded in paraffin). Tumour length maximum diameter and tumour width maximum diameter were outlined. Tumour thickness was calculated as the number of slices containing index tumour multiplied by the average slice thickness of the respective specimen.

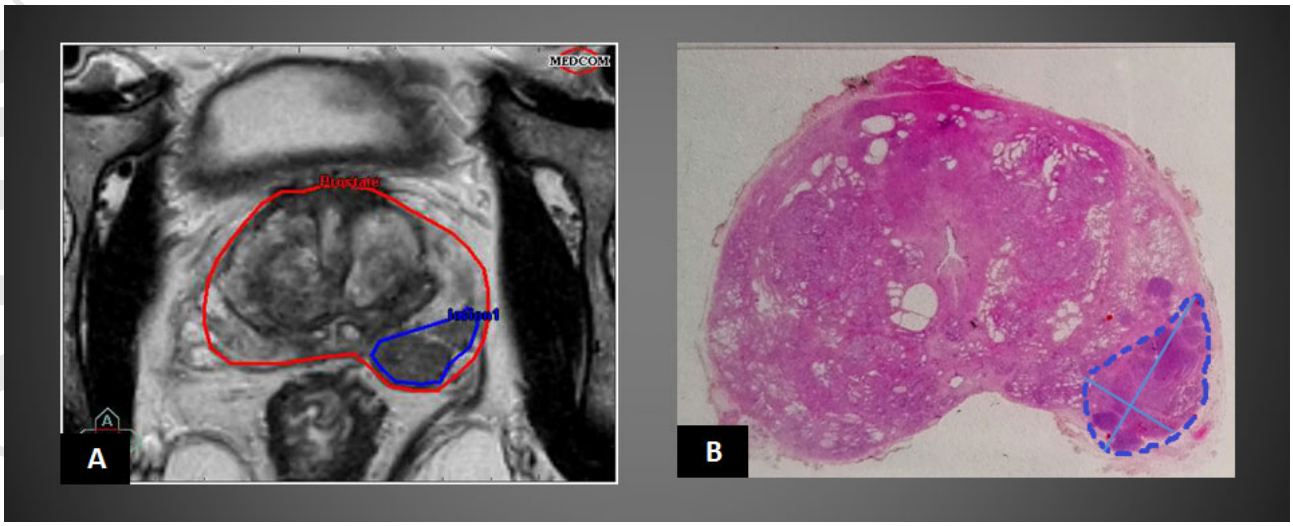

Figure 4. Suspicious lesion affecting the anterior zone of the prostate. In this figure, US/MRI fusion was performed and the obtained MRI VOI was overlapped to the equivalent US scan. Histopathological examination revealed a GS 7 (3+4) prostate cancer in all targeted cores.

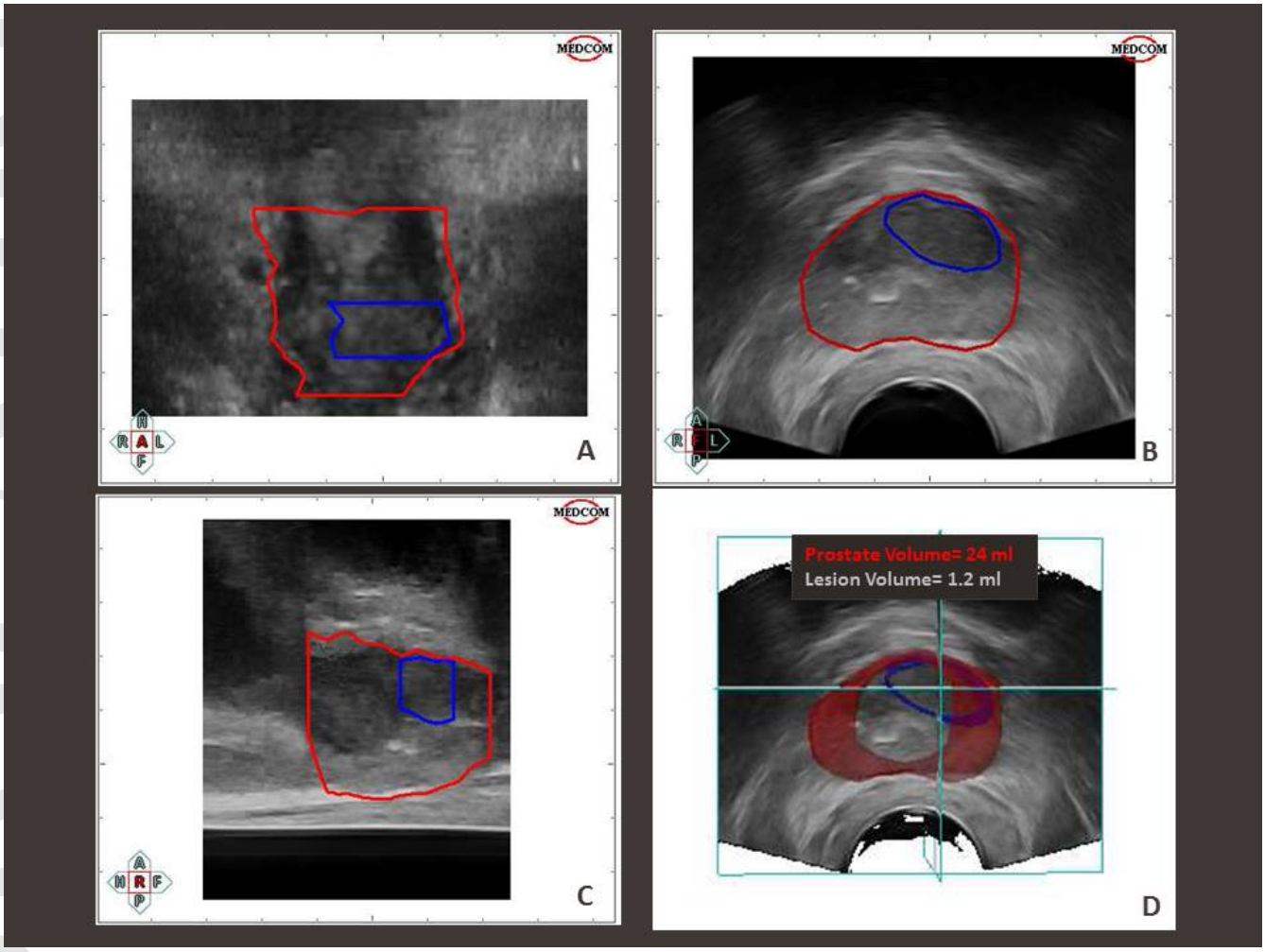

Figure 5. PRO-MAG ultra ®. It is an automatic and reusable biopsy gun for histological core biopsies: A) Needle allocation system; B) Biopsy gun ready for use; C) The needle has an echogenic tip for accurate placement under ultrasound guidance; D) Biopsy core.

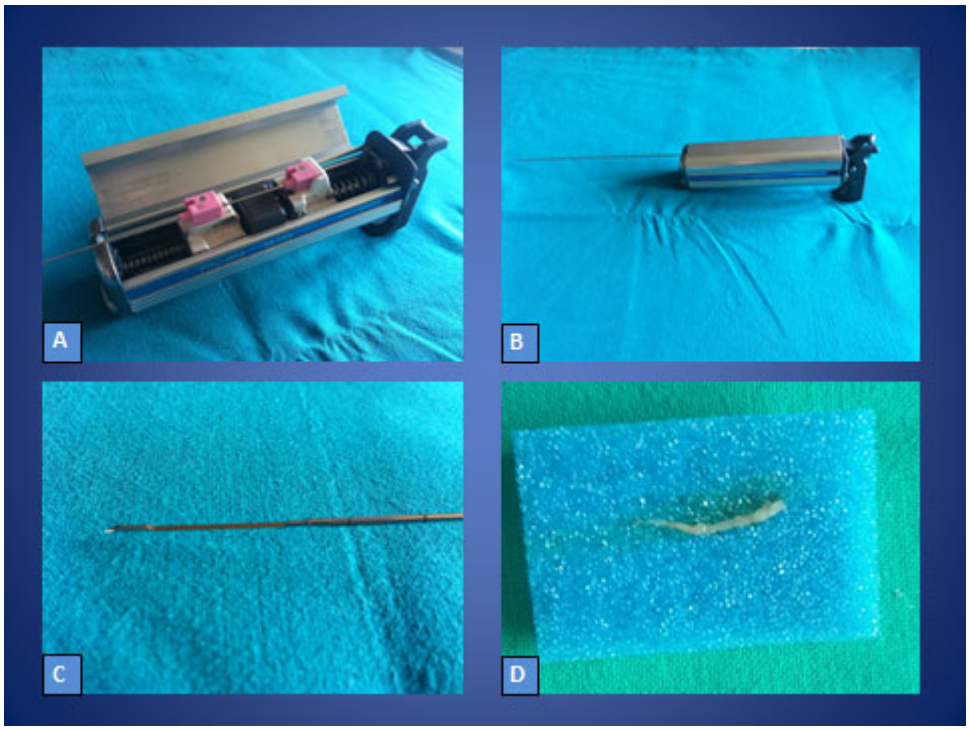

Figure 6. Boxplot representation of LV distribution according with their positive or negative histological results. For negative SL volume median value was 0.37, for positive SL volume median value was 0.59.

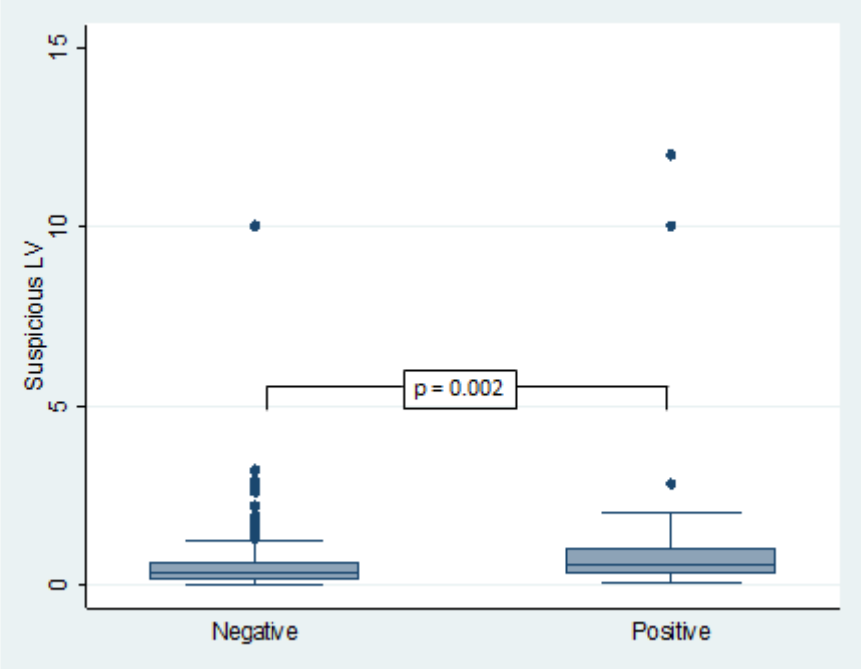

Figure 7. Boxplot representation of LV distribution according with their Gleason Score.

C. LV distribution considering non-aggressive (GS≤6) and aggressive (GS≥7) tumors

D. LV distribution inside each GS groups

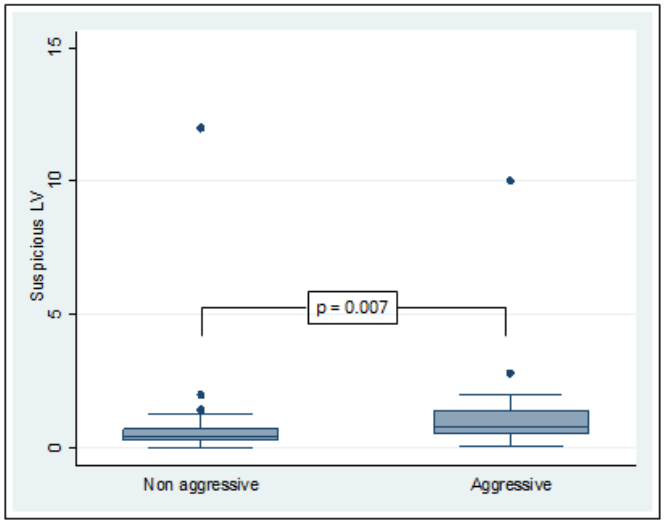

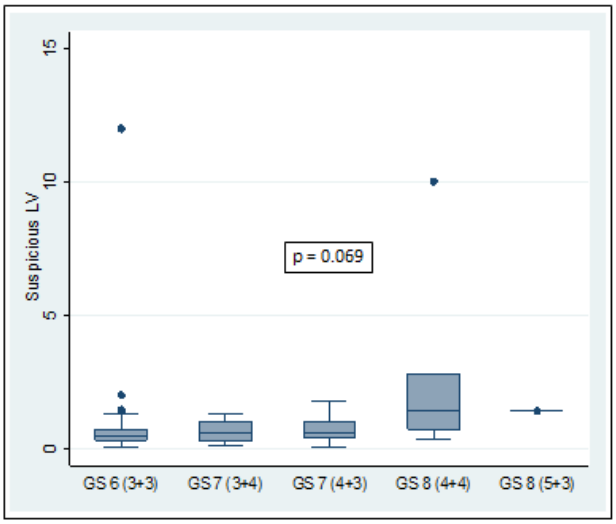

Figure 8. (A) Scatter plot showing correlation between MRI estimated tumor volume (mpMRI LV) and histological tumor volume (HTV) in 23 patients. The red line indicates the regression line. **(B)** Bland-Altman plot showing the limitation of agreement between mpMRI LV and HTV. The orange line represents the linear regression line. The percentage difference between mpMRI LV and HTV is plotted against the average tumor volume (calculated from both mpMRI LV and HTV). All values above the zero line represent overestimation of mpMRI LV, and all values below the zero line represent underestimation of mpMRI LV. The average underestimation of HTV by MRI is 4.2% (95%CI [2% - 8.2%]), and is constant throughout the measurement range. The limit of agreement ranges from -0.54 to +0.15, which indicates clinically significant inaccuracy for mpMRI LV. The median (range) is 0.72 ml (0.12–3.8 ml) for mpMRI LV and 0.89 ml (0.12–4.4 ml) for HTV. Graphic generated using MedCalc Software bvba Version 16.4.3.